



Electrical and Mechanical Performance of Zirconia-Nickel Functionally Graded Materials

M. S. EL-Wazery^{a*}, A. R. EL-Desouky^a, O. A. Hamed^a, A. Fathy^b, N. A. Mansour^c

^a Department of Production Engineering and Mechanical Design, Faculty of Engineering, Menoufiya University, Shebin El-Kom, Egypt

^b Department of Mechanical Design and Production Engineering, Faculty of Engineering, Zagazig University, Egypt

^c Nuclear Research Center, Atomic Energy Authority Cairo, Egypt

PAPER INFO

Paper history:

Received 05 December 2012

Accepted in revised form 24 January 2012

Keywords:

Functionally Graded Materials (FGM)

Powder Metallurgy Technique

Electrical Conductivity

A B S T R A C T

In the present work, six-layered (Zirconia/Nickel) functionally graded materials were fabricated via powder metallurgy technique (PMT). The microstructure, fracture surface and the elemental analysis of the prepared components were studied, and their linear shrinkage, electrical conductivity, fracture toughness and Vickers hardness were evaluated. The results show that the linear shrinkage of the non-graded composites was reduced with the nickel content. The electrical conductivity of the YSZ/Ni was strongly depended on its nickel content. The electrical conductivity as a function of nickel content had a typical 'S' shape curve. Vickers's hardness of YSZ/Ni was lower than that of pure ceramic YSZ and was reduced by decreasing the density of the layer of YSZ/Ni FGM, which was attributed to the pores in intermediate layers in the FGM after sintering stage. Also, the fracture toughness obtained by the non-graded composite increases with an increase in nickel content from 0 % to 50% Ni. The functionally graded materials exhibited a high fracture toughness (31 MPa m^{1/2}) compared to the non-graded composite.

doi: 10.5829/idosi.ije.2013.26.04a.06

1. INTRODUCTION

Functionally graded materials (FGMs) provide novel properties and realize multi-functions that cannot be achieved by monolithic or homogeneous materials [1]. By definition, FGMs are used to produce components featuring engineered gradual transitions in microstructure and/or composition. They accommodate a gradient transition of the properties of different materials from one end to another, where the property mismatch (mechanical, thermal, or electrical) can be reduced to minimum [2-4].

The fabrication process is one of the most important fields in FGM research. A large part of the research work on FGMs has been dedicated to processing and a large variety of production methods have been developed for the processing of FGM. Methods that are capable of accommodating a gradation step include powder metallurgy [5-7], sheet lamination, chemical vapor deposition and coating processes. Jin et al. [8]

investigated the variation of elastic modulus and fabrication of the ZrO₂/NiCr functionally graded materials (FGMs). They found that the elastic moduli clearly decrease with the increase of NiCr, which differ greatly from those predicted by the traditional Mori-Tanaka method. Shahrjerdi et al. [9] have investigated the functionally graded metal-ceramic composite fabricated via pressureless sintering. The pure metallic and ceramic components are Titanium (Ti) and Hydroxyapatite (HA). The properties of all FGM products are characterized by shrinkage, optical microscopy, and Vickers hardness. It was found that the Vickers's hardness of HA/Ti is higher than that of pure microcrystalline Ti and reduces by decreasing the density of the layer of HA/Ti.

In this paper, a detailed experimental investigation was conducted to study the electrical and mechanical performance of Zirconia/Nickel functionally graded materials. The FGMs consisting of ZrO₂ and Ni was fabricated by powder metallurgy. Electrical conductivity and fracture toughness were measured by tests conducted on the homogeneous specimens with different weight percentages of Ni.

¹ * Corresponding Author Email: melwazery@mail.com (M. S. EL-Wazery)

2. MATERIALS AND EXPERIMENTAL PROCEDURES

Commercially available ZrO_2 (3 mol % Y_2O_3) and Ni powders were used as the raw powders to fabricate the FGMs by utilizing the powder metallurgy technique. The YSZ and Ni powders were produced by TOSOH Corporation / Japan and MERK Corporation / USA, respectively. The mean particle sizes of powders were $0.3 \mu m$, $10 \mu m$ for the ZrO_2 and Ni, respectively. The purity of zirconia (3Y-TZ) and nickel were 99 % and 98%, respectively. In this paper, six-layered YSZ/Ni FGM samples were fabricated by powder metallurgy technique as shown in Figure 1. The composition and physical properties of the YSZ and Ni powders are shown in Tables 1 and 2, respectively.

The ZrO_2 and Ni powders were mixed in volume ratios of 10–0, 9–1, 8–2, 7–3, 6–4 and 5–5 and each mixture was suspended in alcohol and milled for five hrs by horizontal ball miller. The ratio of powder to ball was 1:2 and the milling speed was 100 r.p.m. Ethyl alcohol (30wt. %) was added to the mixtures powders to cover the balls.

TABLE 1. Composition of YSZ and Ni

Ni (wt. %)					
Fe	O ₂	Na	C	Co	Ni
0.002	0.12	0.0125	0.1	0.0001	Bal.
ZrO ₂ (3Y-YSZ) (wt. %)					
Y ₂ O ₃	Al ₂ O ₃	SiO ₂	Fe ₂ O ₃	Na ₂ O	ZrO ₂
5.18	0.25	0.008	0.003	0.023	Bal.

TABLE 2. Physical Properties of YSZ and Ni

Raw Materials	Average size (μm)	Melting point($^{\circ}C$)	Density (g/cm^3)	Thermal expansion coefficient 10-6/ $^{\circ}C$
ZrO ₂	0.3	2680	6.05	7
Ni	10	1453	8.90	15.4

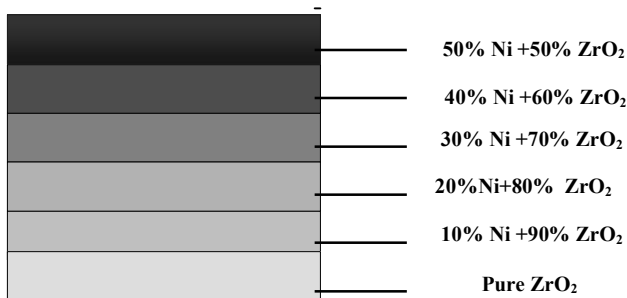


Figure 1. Composition distribution model of the ZrO_2 /Ni FGMs

After milling, the mixed powders were sieved using a $250 \mu m$ steel mesh to remove the remaining agglomerates. 10wt. % ethyl alcohol binder was added to the powders as lubricant. Then, the mixed powders were dried at $70^{\circ}C$ for 24 hrs. The powder blends were put to form a non-graded composition or were layered so as to form graded composition in a rectangular hot work tool steel die with 35 mm length and 10 mm width. The powder compacts were lower pressed up to 5 Pa at room temperature for one minute during the stacking of the layers. The die and punch set-up used to produce the non-graded composites and functionally graded materials (FGM) are reviewed in our first paper [10]. Hydraulic press was used to compact the powder layers once at the same pressure (25 Pa) to press the green compact and obtained the same thickness of the layers. Using same pressing conditions, a larger thickness (6.5 mm) FGM green compact was also formed but under lower pressure during stacking the layers, which would be used for mechanical property testing. The formed functionally graded materials and non graded composite compacts were subjected to pressureless sintering inside a tube furnace under high vacuum pressure (10^{-7} mbar) at $1400^{\circ}C$ for 2 hours to prevent oxidation of nickel (Ni) and the heating rate was $18^{\circ}C/min$ up to $1400^{\circ}C$. Then, the all compacts were cooled inside the tube furnace.

2. 1. Electrical Testing The electrical conductivity of all non-graded composites samples sets were measured at room temperature in air utilizing the two point method. In this method the sintered samples were first cut to rectangular shapes with the dimension of 6 x 7 mm and the thickness of 3 mm. The samples were painted by platinum for connection. Then, the resistance was measured with D.C. RCL (PM6304, Philips) meter at high temperatures up to $800^{\circ}C$. Resistivity and electrical conductivity are calculated by the Equations (1), (2) :-

$$\rho = \frac{A \cdot R}{t} \quad (1)$$

$$\sigma = \frac{1}{\rho} \quad (2)$$

where ρ is the resistivity in $\Omega \cdot cm$, σ is the electrical conductivity in $S \cdot cm^{-1}$, R is the resistance in Ω , and A is the cross sectional area of the sample (axb) in cm^2 , and t is thickness of the sample in cm.

2. 2. Mechanical Testing The variations of fracture toughness (K_{1C}) in the FGMs were investigated directly from the three point-bending tests (3PBT), shown in Figure 2, on the homogenous (non-graded composites) specimens. Fracture tests were conducted on Lloyd LR 10KN universal testing machine at crosshead speed of 0.1 mm/min.

According to ASTM E399-90, an edge crack with the length 1 mm, width 0.3 mm and root radius 0.150 were cut along the mid-span of the fracture specimen utilizing high speed diamond circular saw. Fracture toughness K_{IC} is calculated by the Equation (3).

$$K_{IC} = \frac{3PSY\sqrt{a}}{2WB} \quad (3)$$

where P, S, a, W and B are the fracture load (N), span length, crack size, specimen width and specimen thickness, respectively, and Y is a correction factor of the stress intensity factor and was given as a function of $a/w= 0.33$ [7]. The average fracture toughness for each material composition was taken from three pieces test. The Vickers-indenting positions of the FGM were at the centers of each layer, as illustrated in Figure 3. L_i ($i = 0, 1, 2, 3, 4, 5$) represents the center position of each of the six layers (YSZ and the composite layers from 10 to 50 wt. % nickel). The symbols 0-----5 represent the FGM layers. The distribution of Vickers hardness in the FGMs was directly determined by indenting with a load of 5 kg on each layer of the FGM sample.

2. 3. Materials Characterization The density of the sintered specimens was measured by the water immersion method (Archimedes method); the electrical conductivity was determined by using the RCL meter. The linear shrinkage was measured by a thermal mechanical analyzer (TMA-50 Shimadzu, Japan). The microstructure and the fracture surfaces of some homogeneous specimens were examined by a scanning electron microscope (SEM-JSM 5400). The composition of the selected specimens was determined by the EDX-chart.

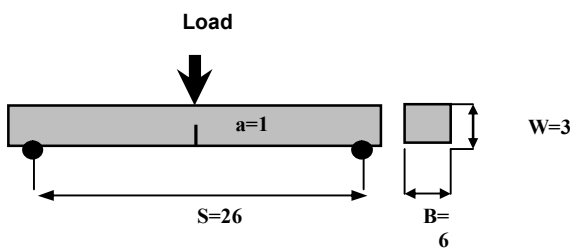


Figure 2. Schematics of the fracture test

Pure ZrO_2	◆	0
$ZrO_2/ 10\% Ni$	◆	1
$ZrO_2/ 20\% Ni$	◆	2
$ZrO_2/ 30\% Ni$	◆	3
$ZrO_2/ 40\% Ni$	◆	4
$ZrO_2/ 50\% Ni$	◆	5

Figure 3. Vickers hardness of the FGM layer

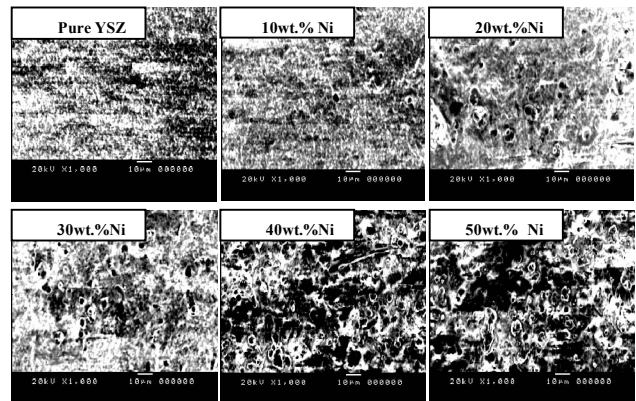


Figure 4. Micrographs of the FGM layers (gray part is nickel in YSZ)

3. RESULTS AND DISCUSSION

3. 1. Microstructure Figure 4 shows the microstructure of the fabricated YSZ/Ni FGM. It has six layers: a pure YSZ layer and five YSZ/Ni composite layers containing, respectively, 10, 20, 30, 40 and 50 % of Ni content. The white and gray regions exhibit the Ni and YSZ phases, respectively.

The white area in each composite shows the nickel phase in a grayish YSZ matrix. The white area increased with increasing Ni contents from 0 to 50 wt.%. Also, it can be seen that metal particles are homogeneously distributed in the ceramic matrix and there is no evidence of agglomerates. As the particle size of the YSZ powder was considerably smaller than that of the Ni powders, YSZ particles would have entered gaps between Ni particles during the fabrication. As a result, the YSZ particles are dispersed in Ni the matrix in the material with high Ni content (40%Ni and 50%Ni).

3. 2. Linear Shrinkage Linear shrinkage is one of the important parameter for evaluating the quality of component gradation in the FGM. Shrinkage could be calculated by accurately measuring the green compact, and then comparing it with the size of the sample after sintering stage. To indirectly estimate the linear shrinkage of the layers in the functionally graded materials fabricated by a pressureless sintering method, the shrinkages of the non-grade composite specimens corresponding to each layer were measured by the TMA instrument and the results were also shown in Figure 5. It could be seen that the maximal value of linear shrinkage among the six layer specimens is 22% for the pure ZrO_2 . The high shrinkage of pure ceramic is mainly due to its lower thermal expansion and hence high sinterability, which leads to high relative density and low level of porosity. Among the five non-graded composite layers, the linear shrinkage decreases with increasing the nickel content and reaches a minimum value of 6% at 50%Ni.

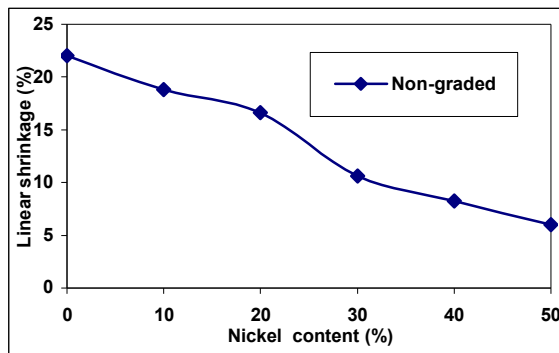


Figure 5. Relation between the linear shrinkage and the nickel content

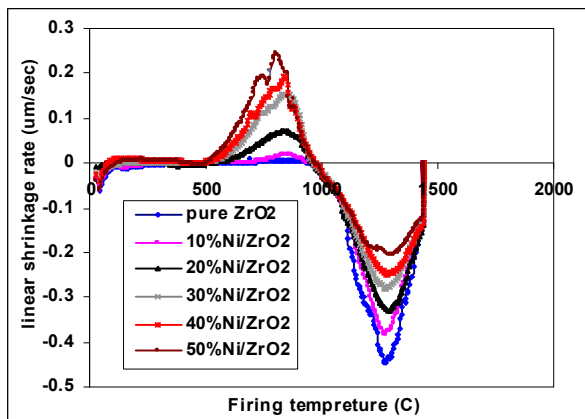


Figure 6. Relation between the linear shrinkage rate with the firing temperature

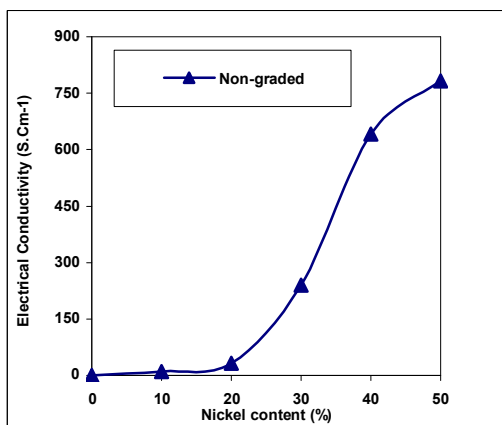


Figure 7. Electrical conductivity as a function of the nickel content

The variations in the linear shrinkage rate with the firing temperature (up to 1400 °C) of the all non-graded composites from 0 % to 50% Ni are shown in Figure 6. From this figure it can be seen that maximum thermal

expansion rate (0.244 $\mu\text{m}/\text{sec}$) of non-graded composites during its firing at 800°C occurs for the 50%Ni/YSZ, also the thermal expansion rate of the all non-graded composites increased with increasing temperature from 29°C to 805°C, then decreased as the firing temperature was increased from 805°C to the neutral point at 973°C. At the neutral point, the thermal expansion rate equals the linear shrinkage rate. The linear shrinkage beyond the neutral point increased with increasing the temperature from 973°C to 1300°C where a maximum linear shrinkage rate for pure ceramic and the all non-graded composites takes place; the rate decreased with the firing temperature up to 1400°C. This is because the ceramic phase (YSZ) exhibited higher sinterability than nickel and the sinterability of the ceramic decreased with increasing nickel content from 0 to 50% Ni.

3. 3. Electrical Conductivity The variation of the electrical conductivity of the sintered YSZ/Ni FGM with the nickel content from 0 to 50% Ni is shown in Figure 7. The conductivity of the YSZ/Ni as a function of nickel content shows the S-shaped curve changing from 0.058 $\Omega\cdot\text{cm}^{-1}$ to 781.79 $\Omega\cdot\text{cm}^{-1}$ predicted by percolation theory [11]. The electrical conductivity of the YSZ/Ni is strongly dependent on its nickel content. The percolation threshold for the conductivity of the YSZ/Ni is about 30 wt.%. This percolation behavior can be explained by the presence of two conduction mechanisms through the YSZ/Ni: an electronic path through the nickel phase and an ionic path through the ceramic phase. The conductivity of 644.34 $\Omega\cdot\text{cm}^{-1}$ was obtained at the point of 40 wt.%. Below the threshold (30 wt% Ni), the YSZ/Ni will behave like an insulator and is similar to that of YSZ due to the fact that the conducting particles are not all connected into a continuous three dimensional network. Above the threshold, the conducting particles are connected leading to a dramatic increase in the YSZ/Ni conductivity. Above 30 wt.% nickel, the conductivity is a bout 3 order of magnitudes higher, corresponding to a change in the mechanism to electronic conduction through the nickel phase. The conductivity of the YSZ/Ni containing more than 30 wt.% Ni depends also on its microstructure (YSZ surface area). At the same nickel content, a support with lower surface area has better nickel particle-to-particle contact, thus higher conductivity for the YSZ/Ni.

3. 4. Fracture Toughness The fracture toughness (K_{1C}) values are plotted versus the material composition of the non-graded composites from 0% to 50% Ni in Figure 8. The fracture toughness of the non-graded composite increases almost linearly with an increase in nickel content from 0% Ni to 50%Ni. The ZrO_2 has relatively low fracture toughness, with a K_{1C} of about 6.60 $\text{MPa}\cdot\text{m}^{1/2}$. The K_{1C} of the non-graded is 9.39

MPa.m^{1/2} for 10 wt.% Ni, and increases up to 15.72 MPa.m^{1/2} for 50 wt.% Ni. This is believed to be the result of the replacement of ceramic phase with poor plastic deformation property with the metal phase with good plastic deformation capability.

The increment in fracture toughness observed in the non-graded composites with higher content of metal inclusions can be assigned to the crack deflection and/or crack extension around the particles. Susceptibility to interface debonding strongly influences the quantitative effect of this micromechanism.

A thermal expansion mismatch exists between the ceramic matrix and the metallic particles. Therefore, internal stresses developed during cooling of the non-graded composites are set up around the metallic inclusions. As the thermal expansion coefficient of the metal is larger than that of the matrix ($\alpha_{Ni} = 15.4 \times 10^{-6} \text{ } ^\circ\text{C}^{-1}$ and $\alpha_{ZrO_2} = 7 \times 10^{-6} \text{ } ^\circ\text{C}^{-1}$), the ceramic-metal interface is subjected to radial tensile stresses. These stresses can produce deflection processes as well as an insufficiently strong interfacial bond which cause the particle debonding as will be shown in the microstructure at 50% Ni. The functionally graded materials FGM exhibited a high fracture toughness (31 MPa.m^{1/2}) than the entire non-graded composite. It is attributed to the low level of porosity and a high relative density.

3. 5. Vickers Hardness The Vickers' hardness of the YSZ/Ni FGM sample was measured using a hardness tester on polished surface under a load of 5 kg (Figure. 9). The averages of five indentations in each layer at the center and the interlayer were used to calculate the hardness values of the layers.

It should be noted that the Vickers hardness decreased with increasing nickel content from 0% to 50%. This is mainly attributed to the pores in intermediate layers in the FGM after sintering stage. The pores are increased in the FGM layers with increasing nickel content and the relative density decreased so that the Vickers hardness was reduced as the transformation from the pure ceramic layer (ZrO₂) to intermediate layers (mixtures of zirconia and nickel powders).

The scanning electron microscope (SEM) micrographs of the fracture surface of the selected non-graded composite after the pressureless sintering are shown in Figure 10. Figure 10(a) shows the SEM micrographs of the notch and fracture surface of the non-graded composite (Ni/YSZ) specimen during the fracture toughness test by using three point bending fixture (3PBF). In addition, non-broken metal particles are observed in the fracture surfaces. Also, there are more dimples resulting from agglomeration of nickel (metal) left in place in 50% non-graded composite as shown in Figure 10(d).

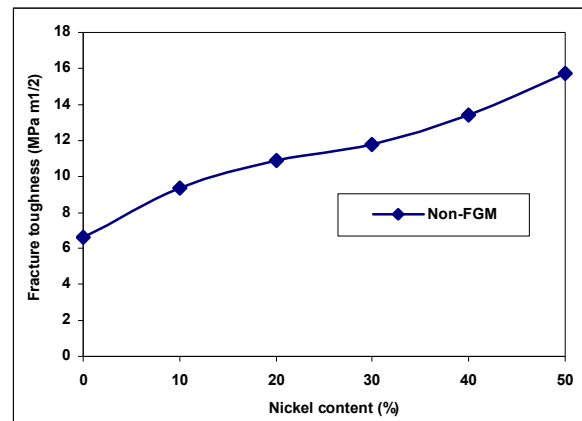


Figure 8. Relation between the fracture toughness and the nickel content

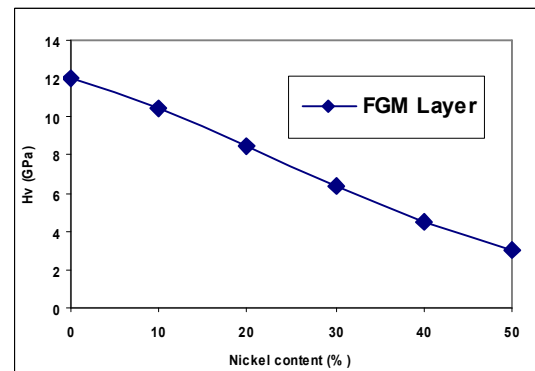
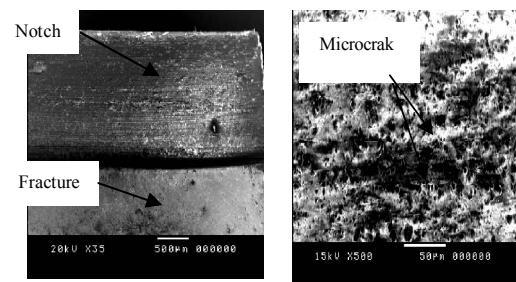


Figure 9. Vickers hardness of the layer in FGM



a) Notch and fracture surfaces of NGC b) 20% Ni NGC

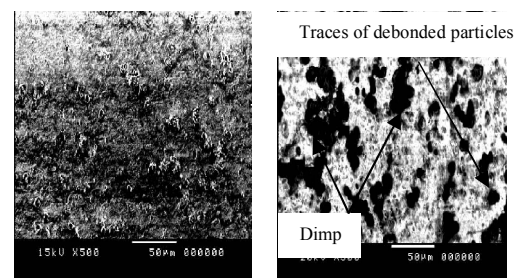


Figure 10. Micrographs of the selected fracture surfaces of the FGM layers

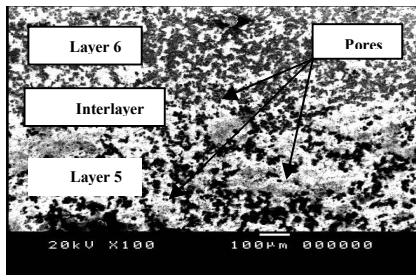


Figure 11. Micrograph of the fracture surface of the FGM interlayer

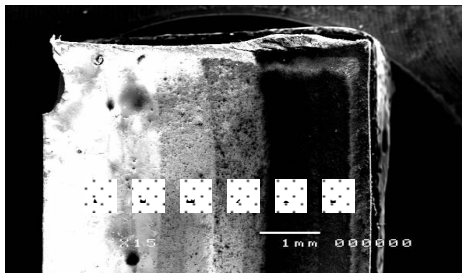


Figure 12. SEM images of the layers in the ZrO₂/Ni FGM (back scatter mode)

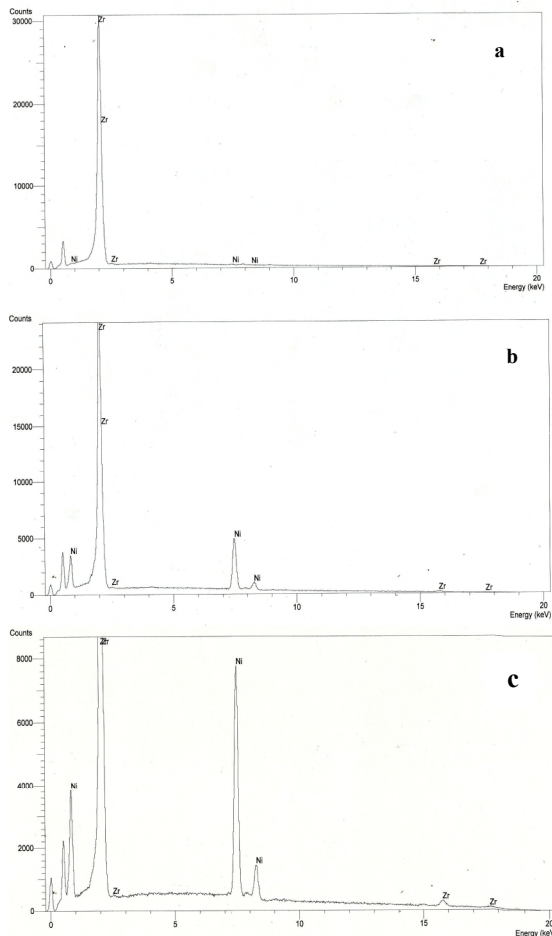


Figure 13. EDX spectra of the FGM layers, a) for layer 1 and b) for layer 4 and c) for layer 6

It is attributed to the change from the brittle phase (ceramic) to the ductile phase (metal). Also, a distinct interface between layer 5 and layer 6 from the fracture surface could be seen in Figure 11. More pores were found in layer 5 (40%Ni/ZrO₂) and increased with increasing nickel content in the layer 6 (50%Ni/ZrO₂). It is attributed to the decrease in sinterability of the intermediate layers, which resulted in a decrease of relative density. The elemental analyses of the layers (1, 4 and 6) in FGM were examined by using an Energy-dispersive X-ray spectroscopy (EDX) coupled with the scanning electron microscope (SEM).

The SEM images of the cross-section of the prepared layers in the FGM components are shown in Figure 12 under the back scatter mode. In the image, it is noted that the light phase in FGM specimens is zirconia and the gray phase is nickel, which is seen quite clearly in the back scattered image.

The compositions in the FGM specimen were further confirmed from the EDX analysis, as shown in Figure 13. The elements in FGM specimen correspond to the compositions of zirconia, mixture of zirconia and nickel. No other elements could be detected from the EDX chart of the layers in the FGM specimens.

4. CONCLUSIONS

The linear shrinkage of the non-graded composites is reduced with the nickel content from 0 to 50% Ni. Also, the electrical conductivity of YSZ/Ni FGM is strongly dependent on its nickel content. The electrical conductivity as a function of nickel content has a typical 'S' shape curve increasing from 0.05 S.cm⁻¹ to 781 S.cm⁻¹ and obvious conductivities were obtained at the 30 wt% Ni.

A percolation threshold for the conductivity of the investigated FGM was found to be at 30wt.% Ni through electronic path via Ni phase and an ionic path via the ceramic phase. Below 30% Ni, FGM behaves like an insulator, whereas above that a dramatic increase in conductivity occurs.

The fracture toughness of the non-graded composite increased from 6.60 to 15.70 MPa.m^{1/2} with an increase in nickel content from 0% to 50%. This is believed to be the result of the variation of ceramic phase with poor plastic deformation property to the metal phase with good plastic deformation property.

Finally, Vickers hardness decreased with increasing nickel content from 0% to 50% Ni. Non-broken metal particles are observed in the fracture surfaces. Also, there are more dimples in the microstructure resulting from agglomeration of nickel (metal) left from place in 50% non-graded composite.

5. REFERENCES

1. Neubrand, A. and Rodel, J., "Gradient materials: an overview of a novel concept", *Zeitschrift für Metallkunde*, Vol. 88, No. 5, (1997), 358-371.
2. Amada, S., "Hierarchical functionally gradient structures of bamboo, barley, and corn", *MRS Bulletin-Materials Research Society*, Vol. 20, No. 1, (1995), 35-36.
3. Hirai, T., Sasaki, M. and Niino, M., "CVD in situ ceramic composites", *Journal of Japan Society of Materials Science*, Vol. 36, No. 410, (1987), 1205-1211.
4. Jin, X., Wu, L., Sun, Y. and Guo, L., "Microstructure and mechanical properties of ZrO₂/NiCr functionally graded materials", *Materials Science and Engineering: A*, Vol. 509, No. 1, (2009), 63-68.
5. Cannillo, V., Lusvarghi, L., Manfredini, T., Montorsi, M., Siligardi, C., and Sola, A., "Glass-ceramic functionally graded materials produced with different methods", *Journal of the European Ceramic Society*, Vol. 27, No. 2, (2007), 1293-1298.
6. He, Z., Ma, J. and Tan, G., "Fabrication and characteristics of alumina-iron functionally graded materials", *Journal of Alloys and Compounds*, Vol. 486, No. 1, (2009), 815-818.
7. Tohgo, K., Iizuka, M., Araki, H. and Shimamura, Y., "Influence of microstructure on fracture toughness distribution in ceramic-metal functionally graded materials", *Engineering Fracture Mechanics*, Vol. 75, No. 15, (2008), 4529-4541.
8. Jin, X., Wu, L., Licheng, G. and Yuguo, S., "Prediction of the variation of elastic modulus in ZrO₂/NiCr functionally graded materials", *Composites Science and Technology*, Vol. 69, No. 10, (2009), 1587-1591.
9. Shahrjerdi, A., Mustapha, F., Bayat, M., Sapuan, S. and Majid, D., "Fabrication of functionally graded Hydroxyapatite-Titanium by applying optimal sintering procedure and powder metallurgy", *International Journal of Physical Sciences*, Vol. 6, No. 9, (2011), 2258-2267.
10. El-Wazery, M., El-Desouky, A., Hamed, O., Mansour, N. and Hassan, A., "Fabrication and Mechanical Properties of ZrO₂/Ni Functionally Graded Materials", *Advanced Materials Research*, Vol. 463, (2012), 463-471.

Electrical and Mechanical Performance of Zirconia-Nickel Functionally Graded Materials

M. S. EL-Wazery ^{a*}, A. R. EL-Desouky^a, O. A. Hamed^a, A. Fathy ^b, N. A. Mansour^c

^a Department of Production Engineering and Mechanical Design, Faculty of Engineering, Menoufiya University, Shebin El-Kom, Egypt

^b Department of Mechanical Design and Production Engineering, Faculty of Engineering, Zagazig University, Egypt

^c Nuclear Research Center, Atomic Energy Authority Cairo, Egypt

چکیده

PAPER INFO

Paper history:

Received 05 December 2012

Accepted in revised form 24 January 2012

Keywords:

Functionally Graded Materials (FGM)

Powder Metallurgy Technique

Electrical Conductivity

در تحقیق حاضر ماده‌ی شش لایه‌ی مرکب (کامپوزیت) تدریجی (اکسید زیرکونیوم/ نیکل) به روش متالورژی پودر ساخته شده است. ریزساختار، سختی سطحی و آنالیز عنصری تر کیپ ساخته شده مورد بررسی قرار گرفته و انقباض خطی، هدایت الکتریکی، چقرمگی شکست و سختی ویکرز ارزیابی شده‌اند. نتایج نشان می‌دهند که انقباض خطی کامپوزیت لایه‌ای با محتوای نیکل کاهش پیدا کرده است. قابلیت هدایت الکتریکی YSZ/Ni به شدت به محتوای نیکل آن وابسته است. قابلیت هدایت الکتریکی به عنوان تابعی از مقدار نیکل نمودار S شکل دارد. سختی ویکرز برای YSZ/Ni از سرامیک خالص YSZ کمتر بوده و با کاهش چگالی لایه‌ی YSZ/Ni FGM به علت تخلخل لایه-ی میانی FGM بعد از تفجوشی کاهش پیدا کرده است. همچنین سختی ساختار به دست آمده از کامپوزیت لایه‌ای با افزایش محتوای نیکل از ۰ تا ۵۰ درصد افزایش پیدا کرده‌است. مواد تدریجی چقرمگی شکست بالاتری (31 MPa $m^{0.5}$) در مقایسه با کامپوزیت‌های لایه‌ای نشان دادند.

doi: 10.5829/idosi.ije.2013.26.04a.06